Development of hydrogel-nanoparticle systems for wound healing

Inês Vitória Duarte
iBB – Institute for Bioengineering and Biosciences, Instituto Superior Técnico
Universidade de Lisboa, Av. Rovisco Pais 1, 1049-001 Lisboa, Portugal
ines.v.duarte@tecnico.ulisboa.pt

***Abstract*—Chronic wounds present a challenging problem, since current therapies are not highly effective, with extended healing time, high recurrence rates and risk of amputations. Insulin is one of the cheapest growth factors available, stimulating wound healing and reducing healing time. However, the harsh proteolytic effect in the wound bed requires a delivery system able to protect insulin from degradation. The aim of this work was to develop an insulin-loaded multifunctional nanoparticle hydrogel delivery system to accelerate wound healing. Insulin-loaded chitosan-coated PLGA nanoparticles were produced by w/o/w double emulsion technique and embedded in hydrogels obtained by freeze-thawing. The delivery system was optimized by quality-by-design approach. Nanoparticles were characterized by dynamic light scattering and scanning electron microscopy, and hydrogels by rheology and FTIR. Insulin structure was evaluated by circular dichroism, and *in vitro* release profile, cell scratch and citotoxicity tests were performed. The nanoparticles showed particle size increase and zeta potential change into positive values, showing an effective chitosan coating. Scanning electron microscopy images showed that nanoparticles incorporated into the hydrogel, maintaining its features with no relevant signs of particle aggregation. The results revealed that insulin structure was preserved upon encapsulation and production of the hydrogel. The nanoparticles embedded in the hydrogel allowed a sustained insulin release of 10% and 25% up to 72h, for the insulin uncoated and chitosan coated nanoparticles, respectively. *In vitro* cell scratch assay did not show enhanced cell migration for the hydrogel-nanoparticle systems developed, but showed enhanced cell migration for the culture medium with insulin, closing the gap at 36h, versus 48h for the other conditions. The cytotoxicity was evaluated and all hydrogels were considered biocompatible. The developed delivery system allows a sustained insulin delivery, protecting its stability and bioactivity and prolonging residence time of insulin in wounds.**

***Index Terms*—Wound healing, Nanoparticle, Hydrogel, Chronic wound, Insulin.**

I. Introduction

The amount of people suffering from chronic wounds (CW) is a growing worldwide health and economic problem due to the increasing prevalence of obesity, chronic diseases, and in general, high-risk population like elderly people [1]. It is believed that 1-2% of the European and United states population are affected by this, and for example, the incidence of diabetic ulcers alone has reached 10-22% of diabetic patients [2], with the number of diabetic people reaching 20 million, and expected to double by 2030, in the USA alone [3]. It is estimated that a single diabetic ulcer comes with a cost of nearly US$50,000 and CW cover as a whole US$25 billion per year. In Europe, the cost related to wound management is 6,000-10,000€ per patient and year [4].

The healing process for acute wounds follows a scheduled pathway composed of four stages: haemostasis, inflammation, proliferation, and remodelling or maturation [2]. This complex process progresses easily for acute wounds, when it is firmly regulated, relying on a balanced molecular environment with growth factors (GF) and cytokines working as the signalling network for the healing process. However, sometimes this balanced molecular environment is non-existing, and not regulated, resulting in non-healing CW [4]. The healing process fails when there is an underlying pathology, like diabetes, tumours, immunodeficiency, venous and arterial insufficiency, and metabolic and connective tissue disorders, that breaks up or stalls the orderly sequence of events for wound healing.

Since the traditional existing treatments cannot guarantee effective healing, with a long-lasting therapy and with a relapse rate of about 70%, it ends up being a heavy socioeconomic burden for the national healthcare systems and the patients [2]. Besides this, patients are at risk of amputations, posing a bigger hurdle to caregivers and the life quality of the patient. The eager for an effective treatment to improve life quality for these patients, and the astonishing budget spend for wound care, are what significantly drives the research for better wound healing(WH) alternatives . Significant efforts have been made in that regard, with the search for new treatments and the improvement of existing ones by understanding the numerous factors involved in normal and pathological tissue repair [2].

One promising strategy is to administer bioactive endogenous compounds, enhancing their bioavailability, to make up for the absence of them in CW bed [4]. These bioactive molecules are either pro-healing molecules and/or suppressors of elevated protease activity [5]. These molecules, for example, could be GF or other bioactive proteins, essential for their biding to specific receptors to activate the cascade of molecular events for WH [4]. Sadly, due to their protein nature, they are easily degraded by the proteolytic environment in CW, requiring frequent administration. To overcome this problem, the molecules can be incorporated in a drug delivery system (DDS), protecting them from protease activity [4].

DDS are technologies engineered for the controlled and targeted delivery of therapeutic agents. The targeted ability of these systems allows local treatment where increased drug concentrations may be beneficial without exposing the body

to high systemic doses of the drug. For topical applications, especially in CW, these systems can improve the patient compliance by delivering an active substance to the wound site and releasing it in a controlled manner for a sustained period of about a week, ultimately solving or minimizing one of the biggest problems of traditional wound treatment [6]. Nanoscale systems have opened new possibilities in this matter. Particularly, using nanoparticles can have several advantages for drug delivery like an increase in drug solubility, prolonged drug release, protect against degradation for bioactive compounds, enhanced bioavailability, and enable a targeted drug delivery while reducing the toxic side effects of the drug [7].

Insulin is an important peptide hormone produced by pancreatic b-cells, that regulates blood glucose levels. Besides being one of the cheapest GF available, insulin is widely used and approved for human use while having no side effects apart from altering blood glucose levels, which has no effect for topical application at low doses [8]. Insulin was reported to promote growth and development of granulation tissue, accelerate reepithelialisation by stimulating migration and proliferation of keratinocytes, stimulate the migration and tube formation of endothelial cells, improving angiogenesis and reducing the healing time [9]. Hence, encapsulating insulin in nanoparticles, protecting them from the peptidase-rich wound environment, and maintaining the bioactivity of insulin could provide all the advantages described above for WH.

II. Material and methods

A. Materials

For the nanoparticles production, it was used poly(lactic-co-glycolic acid) (PLGA) 50:50 Resomer RG 503 H (Mw 24,000-38,000; Tg 44-48°C) from Evonik Industries AG (Essen, Germany), chitosan (low molecular weight 50,000-190,000) and recombinant human insulin from Sigma-Aldrich (St. Louis, EUA), dichloromethane from Thermo Fisher Scientific (Waltham, EUA), hydrochloric acid 1M and Acetic Acid glacial from Panreac (Barcelona, Spain). For the hydrogel production it was used poly(vinyl alcohol) (PVA) (Mw 89,000-98,000) from Sigma-Aldrich, pharmaceutical glycerine from Ceamed (Funchal, Portugal) and sodium alginate from VWR International, LLC (Radnor, EUA). For the insulin structure characterization it was used thioflavin T from Acros organics (Geel, Belgium) and chloroform from Thermo Fisher Scientific. For the high-performance liquid chromatography (HPLC) quantification trifluoroacetic acid and acetonitrile from Thermo Fisher Scientific were used. For the *in vitro* assays the used materials were phosphate-buffered saline (PBS) from Sigma-Aldrich, low-glucose Dulbecco's Modified Eagle's Medium (DMEM) and trypsin from Thermo fischer Scientific, fetal bovine serum (FBS) and antibiotic-antimycotic from Gibco (Waltham, EUA). Milli-Q water was produced in-house and used as the solvent for all solutions.

B. Preparation of insulin-loaded chitosan-coated PLGA nanoparticles

PLGA nanoparticles were produced using a solvent emulsification-evaporation method based on a water-in-oil-in-water (w/o/w) double emulsion technique, previously developed by our group [10]. Briefly, 200mg of PLGA was dissolved in 2mL of dichloromethane. Then, 0.2 mL of an insulin solution with 150mg/ml in HCL 0.1M was added to the polymer solution. The mixture was sonicated for 45 s with 50% amplitude using a Bandelin sonopuls sonicator from Labometer - Sociedade Técnica De Equipamento De Laboratório Lda (Lisbon, Portugal). After sonication, the primary emulsion was poured to 8mL of PVA 2% (w/v) and further sonicated with the same conditions. The final emulsion was added to another 15mL of PVA 2% (w/v) solution and the organic solvent was completely evaporated in constant magnetic stirring using a RT 15 magnetic stirrer from IKA Werke (Staufen, Germany) for 3 hours. For the nanoparticles with chitosan coating, a 1.5% (w/v) chitosan in 1% acetic acid (v/v) solution was prepared. This was added to the nanoparticles solution in different amounts, according to the intended chitosan composition and let to coat for 4 h. The coated nanoparticles were then washed by centrifugation for 20min at 11000 rpm using a Centrifuge 5810 R from Eppendorf International (Hamburg, Germany) and redipersed in 20mL of PVA 2% (w/v). As controls, unloaded nanoparticles both coated and uncoated with chitosan were prepared.

C. Optimization of the nanoparticles-hydrogel formulation

Sodium alginate and glycerin were added to the nanoparticle suspension according to the desired composition, and dissolved in constant magnetic stirring for about 3-4 hours. Then, the formulations were subjected to freeze-thawing cycles, in rounds of 6 hours to freeze, using a freezer at -20°C from Liebherr Group (Bulle, Switzerland), and thaw at room temperature. The optimization of the hydrogel composition was achieved following a quality by design approach using the Statistica software version 10 by TIBCO Software (Palo Alto, USA). The independent variables were the composition of chitosan (0.25, 0.5 and 0.75%), sodium alginate (1, 1.5 and 2%) and glycerin (5, 7.5 and 10%) and the number of freeze-thawing cycles (1, 2 and 3). The effect of these parameters on the product properties was analysed by evaluating the mean particle size and zeta potential, as well as viscosity and spreadability of the hydrogel (dependent variables). The model chosen was a 2**(k-p) standard design with 4 factors (k=4) (independent variables), 1 block (p=1), 8 runs with a triplicate central point and 4 blank columns for the dependent variables. Using the software it was created the matrix with the hydrogel composition for each experiment, and the Design-Expert program, version 6.0.4 by Stat-Ease Inc (Minneapolis, USA), was also used to obtain the optimal hydrogel formulation based on the different compositions.

D. Insulin association efficiency and loading capacity

The amount of insulin carried by the nanoparticles is evaluated by calculating the insulin association efficiency (AE). This calculates the difference between the total amount of insulin used and the amount of free insulin present in the the supernatant after centrifugation, the non-associated insulin. The loading capacity (LC) is calculated as the ratio in percentage between the amount of insulin associated to the nanoparticles and its total weight. The amount of free insulin was assessed by a previously validated reversed-phase HPLC-UV method [11]. Thus, HPLC method was performed using a Waters Corporation (Milford,USA) XTerra RP 18 Column with 4.6mm of diameter, 250 mm of length and pore of 5.0μm and a LiChrospher 100 RP-18 5μm particle size guard column from Merck KGaA (Darmstadt, Germany). The total weight of the nanoparticles is calculated accordingly with the amount of the polymer used to encapsulate insulin. The AE and LC of insulin were determined using the equations (1) and (2), respectively.

$$AE = \frac{Total\ amount\ of\ insulin\ -\ Free\ insulin\ in\ supernatant}{Total\ amount\ of\ insulin} \times 100 \quad (1)$$

$$LC = \frac{Total\ amount\ of\ insulin\ -\ Free\ insulin\ in\ supernatant}{Total\ weight\ of\ nanoparticles} \times 100 \quad (2)$$

E. Particle size and zeta potential analysis

The particles hydrodynamic radius and superficial charge were analysed by dynamic light scattering technique and electrophoretic light scattering, for size and zeta potential analysis, respectively, using a Zetasizer Nano series from Malvern Panalytical (Malvern, United Kingdom). All measurements were performed in triplicate. The gelification ratio was calculated by dividing the mean particle size after gelification by the mean particle size before gelification.

F. Viscosity, spreadability and water content analysis

The viscosity was assessed using a DV-II+Pro Viscometer from AMETEK Brookfield (Middleborough, United States) with the CPE-52 spindle and using a 500 μL sample of the hydrogels until 100%, or close, was reached for torque value. For the spreadability the methodology described by Knorst 1991 [12] was used, with a modification in the sample application mode. The method uses a glass plate with the centre marked, on top of millimetric paper, in which the samples with the same volume (500 μL) were dropped. Predetermined weights of 48.6g, 251.8g and 778g, were put on top of another glass plate, with 1-minute interval. The diameter in opposite directions was measured for all weights, and used to calculated the mean diameter of the hydrogel spread. Three weights were used, and the spreadability (Ei) for each weight was calculated using the following equation: $Ei=d^2(\pi/4)$, where d is the mean diameter. For the water content analysis, weighed samples, of around 1g of hydrogel, were placed in glass vials, previously weighed, and then placed in a Heidolph Instruments (Schwabach, Germany) inkubator 1000 at 66°C for 22 hours. The samples were weighed at 1-hour intervals until a constant weight was reached. The water content was calculated using the following equation:

$$Water\ content\ (\%) = \frac{Hydrogel\ initial\ weight\ -\ Hydrogel\ final\ weight}{Hydrogel\ initial\ weight} \quad (3)$$

G. Scanning electron microscopy

Characterization of the PLGA nanoparticles surface morphology was assessed by scanning electron microscopy (SEM) using an Analytical FEG-SEM: JEOL 7001F microscope from Jeol Ltd. (Tokyo, Japan). The samples were mounted onto metal stubs and vacuum-coated with a layer of gold/palladium before observation in the SEM microscope.

H. Circular dichroism analysis

To assess the insulin structure by circular dichroism (CD), the protein was extracted from PLGA nanoparticles by a treatment using a mixture of chloroform, to dissolve the PLGA from the nanoparticles, with HCl 0.01M to dissolve insulin. The measurements were collected using an π*-180 CD spectrometer from Applied Photophysics (Leatherhead, UK) and Pistar software. The lamp housing was continuously purged with nitrogen at a flow of 8L/min at 25°C. The control protein spectrum was obtained using a 0.2mg/ml solution of insulin in 0.01M HCl. The CD spectra were collected from an average of 3 scans in the 190-250 nm region, with a step of 0.5 nm and averaging time of 5 s using a 0.1 cm cell. The signal was converted to molar ellipticity as θ= CD signal x MRW (mean residual weight of each insulin residue, 116 Da) /(10 x insulin concentration x cell pathlenght). The insulin concentration was determined by UV absorption at 280 nm in a NanoDrop ND-1000 Spectrophotometer from Thermo Fisher Scientific and using a molar extinction coefficient of 5800 $M^{-1}cm^{-1}$.

I. Fluorescence spectroscopy analysis

The extracted protein solution was also used to obtain the fluorescence emission spectra. The spectra were obtained in a 260-400 nm range with 1nm step, with excitation occurring at 280 nm and emission and excitation slits at 10 nm, an averaging time of 0.1 s with a Varian,Inc (Palo Alto, USA) Cary Eclipse Fluorescence Spectrophotometer. The reference spectrum was auto subtracted from the samples spectra and normalized based on the signal intensity.

J. Thioflavin T assay

The extracted protein solution was used to run the thioflavin T experiments in a Varian,Inc (Palo Alto, USA) Cary Eclipse Fluorescence Spectrophotometer. The thioflavin T concentration was 25 μM and insulin was around 11 μM. The samples were excited at 450 nm and the intensity measured at 485 nm with both slit widths at 5 nm, and averaging time of 0.1 s. The reference sample spectrum was subtracted to the test sample. The positive control was a 0.2mg/ml insulin solution heated overnight at 60°C and the negative control was a fresh 0.2mg/ml insulin solution in 0.01M HCl.

K. Fourier Transform Infrared Spectroscopy

The fourier-transform infrared spectroscopy (FTIR) spectra were collected using a Nicolet 5700 FT-IR Spectrometer from Thermo Fisher Scientific with a Smart iTR accessory. The FTIR spectra were obtained by collection of 256 scans with 4cm^{-1} resolution in the 4000-600 cm^{-1} region. All samples were run in triplicate and the average is presented.

L. In vitro Insulin release profile

The insulin-loaded PLGA nanoparticles hydrogel samples were used to evaluate the *in vitro* release profile of insulin. The method used was based in [13]. For this method cell culture inserts from Thermo Fisher Scientific with 8 μm pore size were used since the polycarbonate membrane allows soluble material to pass into the receiver compartment. The hydrogel, previously weight around 1g, was inserted in the inserts. In order to mimic the environment of a wound, the receiver phase was kept at 10mL of pH 7.4 PBS solution and incubated at 33°C under stirring at 150rpm using a Heidolph Instruments Inkubator 1000 and Titramax 1000. The experiment initiated when the inserts containing the hydrogel were suspended in the aqueous receiver phase. Samples of the solution were taken at predetermined time intervals of 0.5h, 1h, 2h, 4h, 8h, 24h, 48h and 72h and fresh medium at the same temperature was replaced to keep the initial volume of the reservoir constant. The collected samples were centrifuged at 13,300 rpm for 30min prior to determination using HPLC methodology. All samples were run in triplicate.

M. In vitro cell scratch assay

Mesenchymal stromal cells (MSC) were cultured with low-glucose DMEM supplemented with 10% (v/v) FBS (FBS MSC qualified) and 1% (v/v)antibiotic-antimycotic (MSC expansion culture medium) and kept at 37°C, 5% CO_2 in a humidified atmosphere. Upon reaching 90% confluence, cells were detached using 0.05% (v/v) Trypsin and counted using the Trypan Blue exclusion method. Cells were sub-cultured into 24-well tissue culture plates at a seeding density of 3000 cells/cm^2. Cells were grown to 100% confluence and scratched using a 200 μL sterile pipette tip. Cells were washed with PBS to remove dead cells and debris, and cultured with the different treatment conditions: A) insulin-loaded chitosan-coated nanoparticle-hydrogel (Ins-Chi-Np-H); B) insulin-loaded nanoparticle-hydrogel (Ins-Np-H); C) chitosan-coated nanoparticle-hydrogel(Chi-Np-H); D) nanoparticle-hydrogel (Np-H); E) Hydrogel; F) MSC expansion culture medium supplemented with insulin 10^{-7} M (CM with insulin) and G) MSC expansion culture medium (culture medium) (2 wells/condition). The conditions A-E were diluted with MSC expansion culture medium (1:20). Cell migration was observed after 24h, 36h and 48h using an Leica DM IL LED microscope with EC3 camera system and the area of cell migration into the scratch was quantified using ImageJ software.

The empty area across the scratch at 0h (a_0) and at each time interval (a_x) were used to calculate the % of empty area in the scratch as (a_x/a_0) x 100.

N. In vitro cytotoxicity assay

The biocompatibility of the hydrogels was demonstrated through a cytotoxicity assay using L929 cell line (mouse fibroblasts) according to ISO10993. The cells were cultured with DMEM supplemented with 10% (v/v) FBS and 1% (v/v) antibiotic-antimycotic (L929 expansion culture medium) and kept at 37°C, 5% CO_2 in a humidified atmosphere. Upon reaching 90% confluence, cells were detached using 0.05% (v/v) Trypsin and counted using the Trypan Blue exclusion method. Cells were sub-cultured into 24-well tissue culture plates at a seeding density of 80,000 cells/cm^2. After 24h, spent culture medium was removed and cells were incubated with the different treatment conditions: A) Ins-Chi-Np-H; B) Ins-Np-H; C) Chi-Np-H; D) Np-H); E) Hydrogel; F) L929 expansion culture medium supplemented with insulin 10^{-7} M(CM with insulin); G) expansion culture medium supplemented with 10% (v/v) DMSO (positive control) and H) L929 expansion culture medium (negative control) (3 wells/condition). The conditions A-E were diluted with L929 expansion culture medium (1:2 and 1:20) 48h prior to cell incubation. After 48h, the treatment conditions were removed and cells were incubated with MTT solution (1mg/ mL) for 2 h. After the incubation period, MTT solvent (HCl and IPA – 1:100) was added and the plates were stirred for 10 min. Absorbance was quantified at 570 nm to determine total cell viability.

III. Results and discussion

A. Nanoparticle-hydrogel optimization

The nanoparticle-hydrogel composition was optimized using a quality by design approach which consisted of varying the concentration of chitosan, alginate and glycerin in the nanoparticle-hydrogel and the number of freeze-thawing cycles. These independent variables were chosen because they are the ones that contribute most for the hydrogel properties and the nanoparticles mucoadhesive properties, which is the main focus of this optimization. For the optimization of the hydrogel all nanoparticles were prepared without insulin. The independent variables were given to Statistica software and the program returned a matrix with 11 formulations, 3 being the central point triplicates. The matrix with the formulations was followed and the different formulations were prepared and characterised by mean nanoparticle size, zeta potential, viscosity and spreadability (dependent variables). The results of these tests were returned to the Statistica program in order to better understand the relations between each independent variable and the dependent variables. The program returned with the relation that each dependent variable had with the independent variables. The sodium alginate was the variable with more statistical significance in the zeta potential, viscosity and spreadability value, and none independent variable was statistical significant in the size of the nanoparticles. The

alginate is the more statistically significant variable because it is the variable that contributes most to the hydrogel properties.

After having the correlations between the independent and dependent variables, the optimal formulation was chosen, with the help of the Design-Expert program. For the sodium alginate was given a goal to maximize its concentration, with a maximum of 2%. This is because the ability of alginate of absorbing excess fluid in the wound bed is very important and it was a property worth maximizing. The glycerin had a goal of keeping in the range of 5-10%. The reason for this is that the function in the hydrogel is to serve as a bodying agent, and therefore, keeping the range allows the program to decide the better concentration for the desired outputs, mainly the viscosity. The chitosan was chosen to maximize in the value of 0.75%, in order to obtain the best muco-adhesion properties possible. The number of cycles was targeted to just one cycle due to energy and time consumption and because this variable did not had a relevant influence with the dependent variables. For the dependent variables of mean particle size and zeta potential both were given the goal of keep the results in range, since all these results were in conformation with what was expected. Since there was certain formulations that did not have an acceptable macroscopic look - less colloidal stability-, the goal for the viscosity was to keep the range of around 1,000-10,000 cP. This is typically the better range for topical application [14], [15] and a range that the results showed to have an acceptable macroscopic look with good colloidal stability. For the spreadability, the goal was to range in between the results obtained previously, since the spreadability does not directly affect the colloidal stability, and so it was let to the program to decide the better glycerin concentration.

Given these constraints, the solution for the optimal formulation given by the program was 2% sodium alginate, 6% glycerin, 0.75% chitosan and 1 freeze-thawing cycle. This composition will be used for the remaining tests ahead, where insulin will be loaded in the nanoparticles.

B. Insulin-loaded nanoparticles Characterization

To begin the insulin-loaded nanoparticle-hydrogel characterization, using the optimal formulation obtained by design of experiments, the effect of insulin association needs to be evaluated in the nanoparticles characteristics. In order to understand the effects of insulin and chitosan in the characterization of the nanoparticles, four experimental groups were used: PLGA nanoparticles (PLGA Np), chitosan-coated PLGA nanoparticles (Chi-PLGA Np), insulin-loaded PLGA nanoparticles (Ins-PLGA Np) and insulin-loaded chitosan-coated PLGA nanoparticles (Ins-Chi-PLGA Np).

For this the mean insulin loaded nanoparticles size, PdI and zeta potential after production were assessed (Fig. 1).

The results show an increase in the diameter for the chitosan coated nanoparticles, when compared to the uncoated. This was expected, since the chitosan attached to the nanoparticles, creating a thicker layer around the surface of the nanoparticles and thus creating an increase in the size of the nanoparticles.

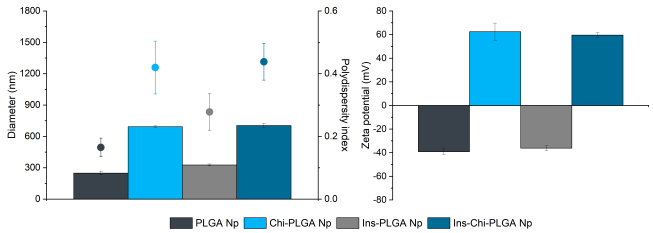

Fig. 1. Mean particle size (left bars), polydispersity index (interval plot) and zeta potential (right bars) characterization of PLGA Np, chitosan-coated PLGA Np, insulin-loaded PLGA Np and insulin-loaded chitosan-coated PLGA Np all with 0.75% chitosan (n=3, mean ± SD).

As showed, the insulin encapsulation did not significantly influence the size of the nanoparticles. The mean particle size values were 248.6±15.7 nm, 693.3±11.4 nm, 326.9±9.0 nm and 704.3±21.2 nm for PLGA nanoparticles, chitosan-coated PLGA nanoparticles, insulin-loaded PLGA nanoparticles and insulin-loaded chitosan-coated PLGA nanoparticles, respectively.

The zeta potential values were -39.2±2.5 mV, 62.5±7.3 mV, -36.2±2.3 mV and 59.6±2.0 mV for PLGA nanoparticles, chitosan-coated PLGA nanoparticles, insulin-loaded PLGA nanoparticles and insulin-loaded chitosan-coated PLGA nanoparticles, respectively. These values show a change in the coated nanoparticles, exhibiting a positive zeta potential, as opposed to the uncoated nanoparticles.

An increase in the size of the nanoparticles with the increase of chitosan concentration indicates that the chitosan attached to the nanoparticles, creating a thicker layer around the surface of the nanoparticles, according to what is described in the literature [16]. The ZP values show a change in the coated nanoparticles, exhibiting a positive zeta potential, as opposed to the uncoated nanoparticles that show a negative zeta potential. These results further corroborate the results from the mean particle size, since the change in negative to positive charge can be explained with the fact that chitosan has a positive charge [17].

The values of polydispersity index (PdI) were low enough to be considered homogeneous samples. The values were 0.165±0.03, 0.420±0.08, 0.278±0.06 and 0.438±0.06 for PLGA nanoparticles, chitosan-coated PLGA nanoparticles, insulin-loaded PLGA nanoparticles and insulin-loaded chitosan-coated PLGA nanoparticles, respectively.

TABLE I
ASSOCIATION EFFICIENCY AND LOADING CAPACITY RESULTS FOR INSULIN-LOADED CHITOSAN-COATED PLGA NP HYDROGEL AND INSULIN-LOADED PLGA NP HYDROGEL (N=3, MEAN ± SD).

Formulation	Association efficiency (%)	Loading Capacity (%)
Ins-Chi-PLGA Np	92.95 ± 1.76	12.12 ± 0.23
Ins-PLGA Np	93.22 ± 0.36	12.15 ± 0.05

In Table I the AE and LC results are presented. The AE was evaluated to assess the insulin association efficiency, an information very important to have in order to know the

amount of insulin in the nanoparticles, especially to use in further tests, like in section III-E, for the insulin release profile. The LC was used to know the insulin loading capacity of the nanoparticles. The association efficiency was above 90% for both formulations, a very good result, taking into account the hydrophilic nature of insulin and hydrophobic polymeric nanoparticles. The results for AE and LC are in conformation to previous studies [18].

C. Insulin-loaded nanoparticle-hydrogel characterization

To continue the insulin-loaded nanoparticle-hydrogel characterization, using the optimal formulation obtained by design of experiments, the effect of insulin association needs to be evaluated in the hydrogel characteristics. In order to understand the effects of insulin and chitosan in the characterization of the hydrogel, five experimental groups were used: insulin-loaded chitosan-coated PLGA nanoparticle-hydrogel (Ins-Chi-PLGA Np-hydrogel), insulin-loaded PLGA nanoparticle-hydrogel (Ins-PLGA Np-hydrogel), chitosan-coated PLGA nanoparticle-hydrogel (Chi-PLGA Np-hydrogel), PLGA nanoparticle-hydrogel (PLGA Np-hydrogel) and hydrogel without nanoparticles (blank hydrogel).

The hydrogel characteristics were evaluated using the gelification ratio and zeta potential after gelification, to evaluate whether the nanoparticle size and zeta potential changed after insulin loading and gelification, and the water content (Table II).

TABLE II
GELIFICATION RATIO, WATER CONTENT AND ZP AFTER GELIFICATION FOR THE DIFFERENT HYDROGEL FORMULATIONS: OF INSULIN-LOADED CHITOSAN-COATED PLGA NP HYDROGEL, INSULIN-LOADED PLGA NP HYDROGEL, CHITOSAN-COATED PLGA NP HYDROGEL, PLGA NP HYDROGEL AND HYDROGEL WITHOUT NANOPARTICLES (N=3, MEAN ± SD).

Formulation	Gelification Ratio	Water content (%)	ZP (mV)
Ins-Chi-PLGA Np-H	0.95 ± 0.13	89.2 ± 0.1	-12.9 ± 1.6
Ins-PLGA Np-H	1.42 ± 0.23	88.6 ± 0.2	-53.0 ± 6.0
Chi-PLGA Np-H	1.27 ± 0.17	89.3 ± 0.2	-9.5 ± 1.3
PLGA Np-H	1.55 ± 0.15	88.7 ± 0.3	-56.1 ± 2.1
Blank hydrogel	-	89.9 ± 0.1	-

In the results given in Table II the gelification ratio was close to the unit in all the formulations, but a bit higher in the formulations without chitosan coating, suggesting that there might have been particle agglomeration in these samples. The fact that the chitosan coated nanoparticles had a gelification ratio closer to 1 further addresses the advantages of the presence of the chitosan coating in the delivery system. The water content in all formulations was around 89%, which was expected for a hydrogel. The high water content is very beneficial to provide a moist environment to the wound bed, promoting tissue regeneration. The zeta potential values are all negative showing a change from positive to negative values in the formulations with chitosan coating that conferred them a positive charge after production, and that now are negative from the alginate present in the hydrogel. The sodium alginate camouflaged the chitosan, changing the surface charge of the nanoparticles. Another interesting find was the fact that the uncoated nanoparticles showed a more negative zeta potential value, which is expected, since these nanoparticles did not had the chitosan to compensate the surface charge to a more positive value.

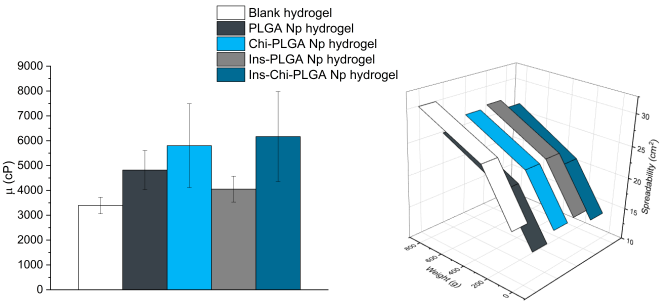

Fig. 2. Viscosity and spreadability after 1 freeze-thawing cycle for blank hydrogel, PLGA Np hydrogel, chitosan-coated PLGA Np hydrogel, insulin-loaded PLGA Np hydrogel and insulin-loaded chitosan-coated PLGA Np hydrogel.

In Fig. 2 the viscosity and spreadability results show that the formulations with chitosan coating were seen to have a tendency of a higher viscosity, although probably not statistically significant. This tendency was not observed in the spreadability of the formulations, with all showing relatively approximate results for the spreadability. All samples showed a proper viscosity range for topical application (1,000-10,000 cP). A macroscopical evaluation was done for the hydrogels. All the formulations look acceptable, with no signs of deposits in the bottom, which conveys good uphold of the nanoparticles in the hydrogel and good colloidal stability. Additionally, the hydrogels with nanoparticles feature a milky aspect, typical from the nanoparticles, and this is not shown in the blank hydrogel.

To evaluate the nanoparticle physiognomy, SEM images where obtained (Fig. 3). To assess the changes that happen when the nanoparticles are embedded in the hydrogel and after the gelification, SEM images where taken in tree different stages of the production process: after production of the nanoparticles (Np after production), nanoparticles embedded in the hydrogel (Np loaded hydrogel), nanoparticles removed from the hydrogel, after gelification (Np in hydrogel).

In the after production phase it is possible to acknowledge that the nanoparticles have a characteristic round shape and smooth surface. It is not possible to see a difference between the different nanoparticles, which indicates that insulin encapsulation does not alter the physiognomy of the nanoparticles. In the nanoparticle loaded hydrogel, although the hydrogel matrix is overlapping the nanoparticles, it is possible to see that the nanoparticles are really well embedded in the hydrogel, which corroborates with the macroscopic assay. In the nanoparticles in hydrogel column, the nanoparticles were removed from the hydrogel in order to assess their conformation after the gelification process. The nanoparticles show no modification comparing to after production, they

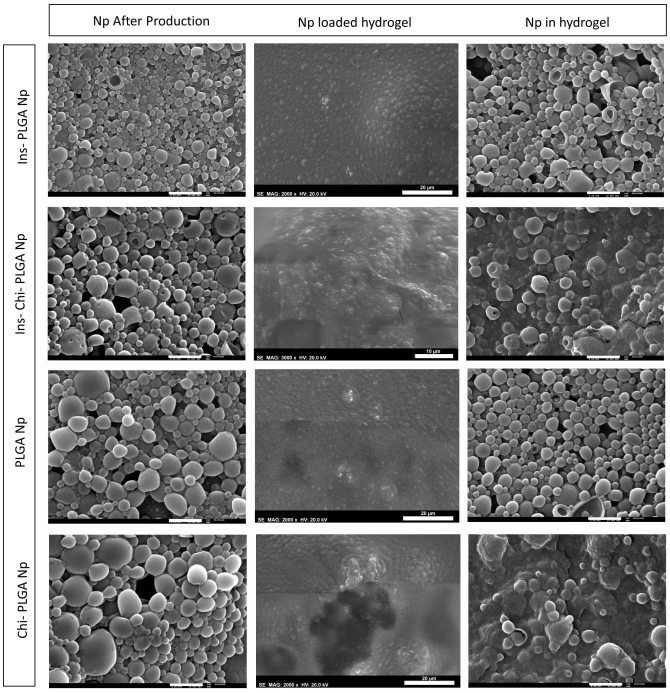

Fig. 3. Nanoparticles-hydrogel SEM images. Insulin-loaded PLGA Np, insulin-loaded chitosan-coated PLGA Np, PLGA Np and chitosan-coated PLGA Np (from top to bottom), after NP production and nanoparticles after gelification with and without hydrogel (left to right). Scale bar: 1 μm for first and third column, 10 μm for second picture of second column and 20 μm for the rest of the second column .

remain round and with a smooth surface, which suggests that the gelification process did not alter the nanoparticles conformation. However, there is a difference to be noted, the nanoparticles coated with chitosan appear to have the chitosan coating still embedded around the nanoparticles. This also means that the chitosan coating remained attached in the nanoparticles after centrifugation for hydrogel removal. This is supported by the presence of a strong electrostatic interaction between the PLGA from the particles and the chitosan coating them, due to their opposite charges - PLGA with negative surface charge and the chitosan with positive. In all the different phases of the production, the nanoparticles maintained their integrity and the size was in accordance with those from Fig. 1.

D. Protein Structure Assessment

Using the insulin extracted from the hydrogel-nanoparticle, the insulin structure and its bioactivity were assessed. In order to test the secondary structure of insulin, CD spectroscopy was performed (Fig. 4).

The reference spectra used is native insulin at 0.2 mg/ml. In this, two minima were observed at 208.5 and 222 nm, which are distinct of the α-helix structure of the protein [19]. A maximum was also observed at 197 nm. This spectra is in accordance with other described by research works [20].

The CD spectra from the samples showed a similar shape of the curve, with the two minina and maximum at about

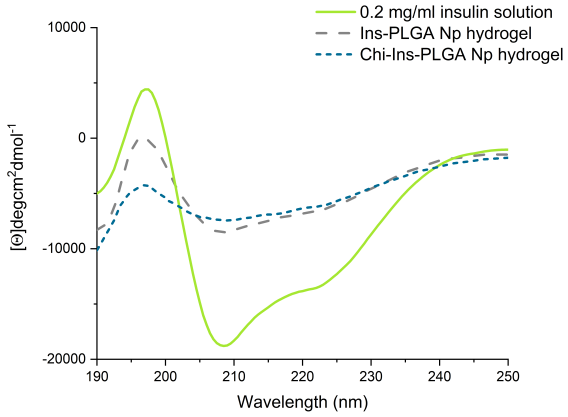

Fig. 4. Far-UV CD spectra of insulin extracted from insulin-loaded PLGA nanoparticles hydrogel and insulin-loaded chitosan-coated PLGA nanoparticles hydrogel. Insulin 0.2 mg/mL in 0.01 HCl used as reference.

the same wavelength. Maximum at 197 nm for both samples, and minima at 209 and 222.5 nm for Ins-PLGA nanoparticle hydrogel and 208.5 and 221.5 nm for Chi-Ins-PLGA nanoparticle hydrogel. These results show no relevant changes in the α-helix structure.

As for the β-sheets, these are predominant if denaturation, aggregation or even fibrillation of insulin occurs. It is possible to observe this presence of β-sheets with a characteristic minima of ellipticity at around 216 nm [21]. Considering this is not observed in Fig. 4, the structural modifications from α-helix into β-sheets did not occur, so it is predicted that the insulin extracted from the hydrogel-nanoparticle formulations maintained its secondary structure and bioactivity.

The differences observed in the CD spectra are related to the ellipticity signal, which represents some change in the spatial conformation of the protein. This is to be expected since the insulin extracted from the nanoparticles is exposed to some invasive procedures, like the production of the nanoparticles and hydrogel, and the extraction in itself. Besides the presence of this insulin conformation change, the maintenance of the minina suggest that the insulin maintained its bioactivity.

Thioflavin T assay results (data not shown) showed no signal enhancement, which means no presence of thioflavin T positive filaments or formation of amyloid fibrils. The positive control showed signal enhancement which is expected since this was fibrillated insulin. These results show that the production method maintained the insulin structure stable.

Fluorescence spectroscopy was also used to assess the structure of insulin extracted from PLGA nanoparticle-hydrogel system (Fig. 5). Insulin fluorescence depends on its four tyrosine residues, hence alterations in the intensity of the emission spectra of insulin are indicators of conformation modification [22].

In the reference spectrum, and for the sample spectra a maximum was observed at 284 nm. This maximum is shifted when compared to the literature [23], however when

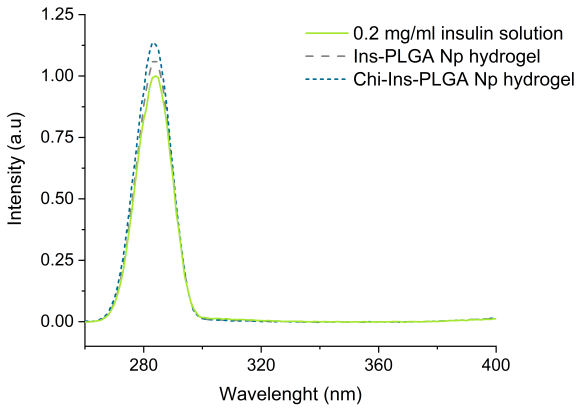

Fig. 5. Fluorescence spectra of insulin extracted from insulin-loaded PLGA nanoparticles hydrogel and insulin-loaded chitosan-coated PLGA nanoparticles hydrogel. Insulin 0.2 mg/mL in 0.01 HCl used as reference.

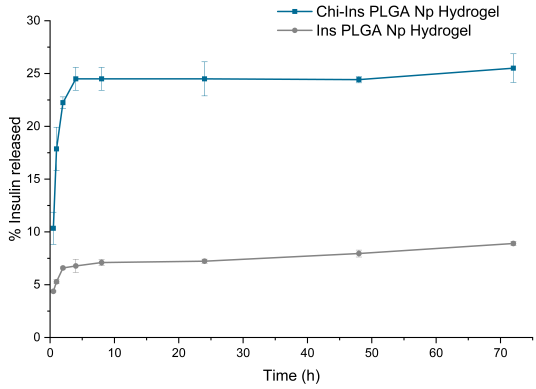

Fig. 6. Insulin release profile from insulin-loaded chitosan-coated PLGA nanoparticles hydrogel and insulin-loaded PLGA nanoparticles hydrogel.

comparing between the reference insulin spectrum and the samples spectra there is no shift in the maxima, which is an indication of the preservation of insulin structure. However there are some differences regarding the increase in intensity observed, which hints to some conformational changes [24]. Insulin from Ins-PLGA nanoparticle hydrogel showed higher intensity and insulin from Chi-Ins-PLGA nanoparticle hydrogel showed even higher intensity when compared to native insulin spectrum. Again, expected results due to the stress exposure of the insulin extracted from the samples. Overall, the results indicate a stable structure, and are in agreement with previous structural characterization results from CD and thioflavin T assay.

E. In vitro insulin release profile

To obtain an insulin release profile, the hydrogels containing insulin loaded nanoparticles, insulin-loaded chitosan-coated PLGA nanoparticles hydrogel (Chi-Ins PLGA Np-Hydrogel) and insulin-loaded PLGA nanoparticles hydrogel(Ins PLGA Np-Hydrogel), were used in a release profile methodology for up to 72h. These results were obtained in order to understand the release rate of insulin from the nanoparticles embedded in the hydrogel (Fig. 6).

The insulin release profile shows the cumulative insulin release up to 72h, for the insulin-loaded chitosan-coated PLGA nanoparticle hydrogel and insulin-loaded PLGA nanoparticle hydrogel. The release pattern for both formulations is similar, with the difference in the amount of insulin released. The initial burst effect of insulin release in the first 4h is related to the existence of insulin in the surface of the nanoparticles, which facilitates the diffusion to the medium. From that moment on, the release of insulin is more controlled and steady. Until the 72h a sustained release pattern is observed, reaching about 10 and 25 % for insulin-loaded chitosan-coated PLGA nanoparticle hydrogel and insulin-loaded PLGA nanoparticle hydrogel, respectively. The pattern also indicates that the release of insulin should continue past the 72h, but it is not possible to confirm, without data with more time. The results also indicate that the nanoparticles with chitosan-coating released more insulin over time than the ones without. The reason for this is probably the higher muco-adhesive properties from the chitosan coating, that enables a more intimate interaction between the nanoparticles and the insert membrane, which promotes a greater insulin release. This particular result demonstrates the advantage of using chitosan coating in this delivery system. Furthermore, when comparing this release assay with others from insulin-loaded PLGA nanoparticles without the hydrogel [10], where the insulin was 100% released over 48h, the very obvious difference is the amount the insulin released. When the hydrogel is not present, the nanoparticles are free from the hydrogel matrix, and can release the insulin with more ease. Having the nanoparticles embedded in the hydrogel creates barrier for the release of insulin, which can be advantageous, if a more controlled and sustained release is needed.

F. Cell Scratch assay

To investigate the bioactivity of the insulin and the hydrogels with the nanoparticles, cell scratch assay was performed in MSC (Fig. 7 and 8). The area of the scratch was measured at the beginning of the experiment at 24, 36 and 48h.

The scratch assay provides a measure of cell migration, a critical process for wound healing. The results show that insulin strongly stimulated cell migration, being the only condition that at 24h showed around 90% of the scratch closed and full closure at 36h. For all other conditions cell migration was not as evident, or significantly different between conditions. It was expected that the nanoparticles loaded with insulin would induce cell migration as well, but this was not observed. As seen in section III-D, the insulin from the nanoparticles seemed to conserve its secondary structure, which should also indicate its bioactivity. Knowing this, the probable justification for the fact that the Ins-Chi-Np-H and Ins-Np-H conditions did not showed enhanced cell migration, when compared to the control conditions, could be that the

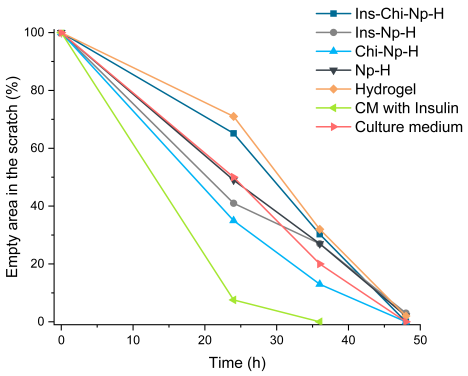

Fig. 7. MSC cell scratch repair assays for evaluation of insulin's bioactivity from Ins-Chi-Np-H, Ins-Np-H, Chi-Np-H, Np-H, Hydrogel, MSC expansion culture medium supplemented with insulin 10^{-7} M and MSC expansion culture medium. CM stands for culture medium.

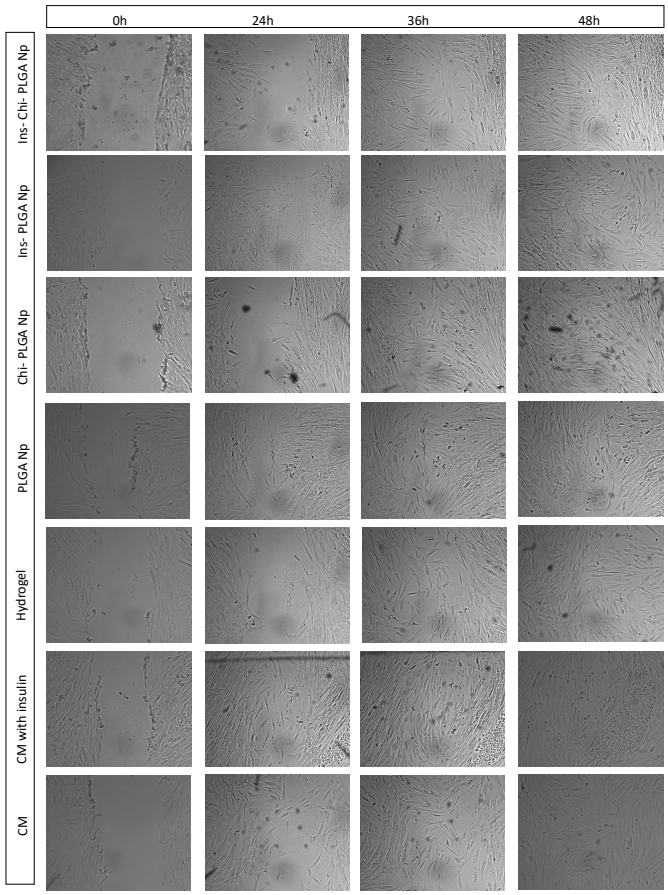

Fig. 8. MSC cell scratch repair assays from Ins-Chi-Np-H, Ins-Np-H, Chi-Np-H, Np-H, Hydrogel, MSC expansion culture medium supplemented with insulin 10^{-7} M and MSC expansion culture medium. CM stands for culture medium.

insulin release from the nanoparticles, as seen in section III-E, was not sufficient to induce cell migration. As seen in the insulin release assay, the insulin released in the Ins-Chi-Np-H and Ins-Np-H reached a maximum of 25 and 10 % at 72h, which was lower than previously observed for these nanoparticles without the hydrogel.

G. Cytotoxicity assay

To assess the biocompatibility of the developed delivery system, a citotoxicity assay was performed. The cell viability % for each condition and concentration, 1:2 and 1:20, are shown in Table III.

TABLE III
L929 CELL VIABILITY % AT DIFFERENT CONCENTRATIONS, 1:2 AND 1:20 AND AT DIFFERENT CONDITIONS: INS-CHI-NP-H, INS-NP-H, CHI-NP-H, NP-H, HYDROGEL, L929 EXPANSION CULTURE MEDIUM SUPPLEMENTED WITH INSULIN 10-7 M, EXPANSION CULTURE MEDIUM SUPPLEMENTED WITH 10% (V/V) DMSO (POSITIVE CONTROL) AND L929 EXPANSION CULTURE MEDIUM (NEGATIVE CONTROL). CM STANDS FOR CULTURE MEDIUM.

Conditions	**Viability (%)**	
	1:2	1:20
Ins-Chi-Np-H	42	86
Ins-Np-H	43	80
Chi-Np-H	68	84
Np-H	53	78
Hydrogel	34	78
CM with insulin	97	
CM with DMSO (+control)	23	
CM (-control)	100	

The culture medium was used as a negative control, where 100% of the cells maintain their viability, and this value is used for comparison to other conditions. Cell viability reduced to less than 70% of the negative control is considered to have a cytotoxic potential. The culture medium with insulin showed great biocompatibility, which was expected. For the different hydrogels, in the concentration of 1:2, 5ml of culture + 5ml of hydrogel, all hydrogels showed cytotoxic potential. In contrary, for 1:20 concentration, all hydrogels showed biocompatibility. Cell viability was similar for the chitosan-coated nanoparticles, Ins-Chi-Np-H and Chi-Np-H with 86 and 84%, respectively, and similar for the other formulations, Ins-Np-H, Np-H and hydrogel with 80, 78 and 78%, respectively. The slight increase in cell viability for the formulations with chitosan, could be explained by the presence of the natural polymer, chitosan, which is known to have great biocompatibility owing to the similarity to macromolecules recognised by the human body.

IV. CONCLUSIONS

This research aimed to develop a DDS to aid in chronic WH. The optimization process for he nanoparticle-hydrogel revealed an optimal formulation with 2% sodium alginate, 6% glycerin, 0.75% chitosan and 1 freeze-thawing cycle. This composition was used for the remaining formulations with insulin loading. The nanoparticles maintained its features after production and gelification. The results revealed that insulin structure was preserved upon encapsulation and production of the hydrogel and the DDS allowed a sustained insulin release up to 72h. All hydrogels were considered biocompatible.

It is important to point out the importance of continuing this research work whether to optimize the production of the DDS or to continue with *in vitro* or *in vivo* testing. The *in vitro* release assay should also be revised, since the methodology had some difficulties related to the little amount of receiver phase. Mainly, to obtain information of the total time it takes for 100% of the insulin to be released, it would be a good idea to extend the period of time of the assay. Having that information would be advantageous to fully understand the controlled and sustained release of insulin in this approach, and further investigate the frequency of dressing changes for *in vivo* testing.

For the *in vitro* cell scratch, based on the results, it should be considered a revision on the time at which measures of the empty area of the scratch are made. The reason for this is that at 48h all the gaps are closed, and from the beginning only tree time points are measured. Since the scratches rapidly closed, it would be beneficial to have more information on what happens between 0 and 24h, for example. Another suggestion would be to repeat the assay with the nanoparticles without the hydrogel, to understand the results obtained. The fact that none the insulin-loaded nanoparticles system had the ability of enhancing cell migration, could be explained with the repetition of this test but without the hydrogel. To comprehend if the hydrogel does act as a barrier for the insulin release, and therefore insulin-like effects could not be seen in cell migration, or if the insulin released lost its bioactivity and therefore insulin advantages were lost.

Finally, *in vitro* testing does not replace *in vivo* tests, since *in vitro* never truly acts like a living being, it only mimics parts of it. For this reason, further research in *in vivo* models is needed to fully comprehend the effectiveness of this approach.

V. Ackowledgement

This document was written and made publically available as an institutional academic requirement and as a part of the evaluation of the MSc thesis in Biological Engineering of the author at Instituto Superior Técnico. The work described herein was performed at the Institute for Bioengineering and Biosciences (iBB) of Instituto Superior Técnico (Lisbon, Portugal), during the period March-November 2020, under the supervision of of Prof. Pedro Fonte and Prof. Duarte Miguel Prazeres, and advisership by Prof. Ana Macedo.

References

[1] A. J. Whittam, Z. N. Maan, D. Duscher, V. W. Wong, J. A. Barrera, M. Januszyk, and G. C. Gurtner, "Challenges and opportunities in drug delivery for wound healing," *Advances in Wound Care*, vol. 5, no. 2, pp. 79–88, 2016.

[2] W. Wang, K.-j. Lu, C.-h. Yu, Q.-l. Huang, and Y.-Z. Du, "Nano-drug delivery systems in wound treatment and skin regeneration," *Journal of Nanobiotechnology*, vol. 17, no. 1, p. 82, 2019.

[3] G. Han and R. Ceilley, "Chronic wound healing: a review of current management and treatments," *Advances in Therapy*, vol. 34, no. 3, pp. 599–610, 2017.

[4] I. Garcia-Orue, J. L. Pedraz, R. M. Hernandez, and M. Igartua, "Nanotechnology-based delivery systems to release growth factors and other endogenous molecules for chronic wound healing," *Journal of Drug Delivery Science and Technology*, vol. 42, pp. 2–17, 2017.

[5] V. R. Krishnaswamy, M. Manikandan, A. K. Munirajan, D. Vijayaraghavan, and P. S. Korrapati, "Expression and integrity of dermatopontin in chronic cutaneous wounds: a crucial factor in impaired wound healing," *Cell and Tissue Research*, vol. 358, no. 3, pp. 833–841, 2014.

[6] J. S. Boateng, K. H. Matthews, H. N. Stevens, and G. M. Eccleston, "Wound healing dressings and drug delivery systems: a review," *Journal of Pharmaceutical Sciences*, vol. 97, no. 8, pp. 2892–2923, 2008.

[7] S. Parveen, R. Misra, and S. K. Sahoo, "Nanoparticles: a boon to drug delivery, therapeutics, diagnostics and imaging," *Nanomedicine: Nanotechnology, Biology and Medicine*, vol. 8, no. 2, pp. 147–166, 2012.

[8] T. Emanuelli, A. Burgeiro, and E. Carvalho, "Effects of insulin on the skin: possible healing benefits for diabetic foot ulcers," *Archives of Dermatological Research*, vol. 308, no. 10, pp. 677–694, 2016.

[9] A. Oryan and E. Alemzadeh, "Effects of insulin on wound healing: a review of animal and human evidences," *Life Sciences*, vol. 174, pp. 59–67, 2017.

[10] P. Fonte, S. Soares, A. Costa, J. C. Andrade, V. Seabra, S. Reis, and B. Sarmento, "Effect of cryoprotectants on the porosity and stability of insulin-loaded plga nanoparticles after freeze-drying," *Biomatter*, vol. 2, no. 4, pp. 329–339, 2012.

[11] B. Sarmento, A. Ribeiro, F. Veiga, and D. Ferreira, "Development and validation of a rapid reversed-phase hplc method for the determination of insulin from nanoparticulate systems," *Biomedical Chromatography*, vol. 20, no. 9, pp. 898–903, 2006.

[12] M. T. Knorst, *Desenvolvimento tecnológico de forma farmacêutica plástica contendo extrato concentrado de Achyrocline satureioides (Lam.) DC. Compositae (marcela)*. Master's thesis, Universidade Federal do Rio Grande do Sul, 1991.

[13] R. G. Loughlin, M. M. Tunney, R. F. Donnelly, D. J. Murphy, M. Jenkins, and P. A. McCarron, "Modulation of gel formation and drug-release characteristics of lidocaine-loaded poly (vinyl alcohol)-tetraborate hydrogel systems using scavenger polyol sugars," *European Journal of Pharmaceutics and Biopharmaceutics*, vol. 69, no. 3, pp. 1135–1146, 2008.

[14] L. Buhse, R. Kolinski, B. Westenberger, A. Wokovich, J. Spencer, C. W. Chen, S. Turujman, M. Gautam-Basak, G. J. Kang, A. Kibbe, *et al.*, "Topical drug classification," *International Journal of Pharmaceutics*, vol. 295, no. 1-2, pp. 101–112, 2005.

[15] P. K. Bolla, B. A. Clark, A. Juluri, H. S. Cheruvu, and J. Renukuntla, "Evaluation of formulation parameters on permeation of ibuprofen from topical formulations using strat-m® membrane," *Pharmaceutics*, vol. 12, no. 2, p. 151, 2020.

[16] B.-S. Kim, C.-S. Kim, and K.-M. Lee, "The intracellular uptake ability of chitosan-coated poly (d, l-lactideco-glycolide) nanoparticles," *Archives of Pharmacal Research*, vol. 31, no. 8, p. 1050, 2008.

[17] M. do Céu Teixeira, A. Santini, and E. B. Souto, "Delivery of antimicrobials by chitosan-composed therapeutic nanostructures," in *Nanostructures for Antimicrobial Therapy*, pp. 203–222, Elsevier, 2017.

[18] P. Fonte, F. Andrade, C. Azevedo, J. Pinto, V. Seabra, M. van de Weert, S. Reis, and B. Sarmento, "Effect of the freezing step in the stability and bioactivity of protein-loaded plga nanoparticles upon lyophilization," *Pharmaceutical Research*, vol. 33, no. 11, pp. 2777–2793, 2016.

[19] S. M. Kelly, T. J. Jess, and N. C. Price, "How to study proteins by circular dichroism," *Biochimica et Biophysica Acta (BBA)-Proteins and Proteomics*, vol. 1751, no. 2, pp. 119–139, 2005.

[20] Z. Yong, D. Yingjie, W. Xueli, X. Jinghua, and L. Zhengqiang, "Conformational and bioactivity analysis of insulin: Freeze-drying tba/water co-solvent system in the presence of surfactant and sugar," *International Journal of Pharmaceutics*, vol. 371, no. 1-2, pp. 71–81, 2009.

[21] M. Bouchard, J. Zurdo, E. J. Nettleton, C. M. Dobson, and C. V. Robinson, "Formation of insulin amyloid fibrils followed by ftir simultaneously with cd and electron microscopy," *Protein Science*, vol. 9, no. 10, pp. 1960–1967, 2000.

[22] I. B. Bekard and D. E. Dunstan, "Tyrosine autofluorescence as a measure of bovine insulin fibrillation," *Biophysical Journal*, vol. 97, no. 9, pp. 2521–2531, 2009.

[23] M. Correia, M. T. Neves-Petersen, P. B. Jeppesen, S. Gregersen, and S. B. Petersen, "Uv-light exposure of insulin: pharmaceutical implications upon covalent insulin dityrosine dimerization and disulphide bond photolysis," *PLoS One*, vol. 7, no. 12, p. e50733, 2012.

[24] J. R. Lakowicz, *Principles of fluorescence spectroscopy*. Springer, Boston, MA, 3 ed., 2006.